Monte Carlo Information-Reuse Approach to Aircraft Conceptual Design Optimization Under Uncertainty

Leo W. T. Ng* and Karen E. Willcox†
Massachusetts Institute of Technology, Cambridge, Massachusetts 02139

DOI: 10.2514/1.C033352

This paper develops a multi-information source formulation for aerospace design under uncertainty problems. As a specific demonstration of the approach, it presents the optimization under uncertainty of an advanced subsonic transport aircraft developed to meet the NASA $N + 3$ goals and shows how the multi-information source approach enables practical turnaround time for this conceptual aircraft optimization under uncertainty problem. In the conceptual design phase, there are often uncertainties about future developments of the underlying technologies. An aircraft design that is robust to uncertainty is more likely to meet performance requirements as the technologies mature in the intermediate and detailed design phases, reducing the need for expensive redesigns. In the particular example selected here to present the new approach, the multi-information source approach uses an information-reuse estimator that takes advantage of the correlation of the aircraft model in the design space to reduce the number of model evaluations needed to achieve a given standard error in the Monte Carlo estimates of the relevant design statistics (mean and variance). Another contribution of the paper is to extend the approach to reuse information during trade studies that involve solving multiple optimization under uncertainty problems, enabling the analysis of the risk–performance tradeoff in optimal aircraft designs.

Nomenclature

$A(\omega)$	=	random variable representing the output quantity of interest
a_i, c_i	=	ith sample of the random variables $A(\omega)$ and $C(\omega)$, respectively
$\bar{a}_n$, $\bar{c}_n$	=	regular Monte Carlo estimators for the expectation of random variables $A(\omega)$ and $C(\omega)$, respectively, using n samples
b_i	=	ith sample in the one-pass algorithm for computing the variance
$C(\omega)$	=	auxiliary random variable used as the control variate by the information-reuse estimator
$\mathbb{E}[A(\omega)]$	=	expectation of random variable $A(\omega)$
f	=	objective function for the general optimization under uncertainty problem
$\hat{f}$, $\hat{g}$	=	estimators of f and g, respectively, by replacing the statistic of interest with an estimator
g	=	inequality constraint function for the general optimization under uncertainty problem
k	=	index for the current optimization iteration
ℓ	=	index for the past optimization iteration used by the information-reuse estimator
M	=	numerical model for the optimization under uncertainty problem
n	=	number of samples
n_{init}	=	initial number of samples
p	=	amount of computational effort in terms of the number of model evaluations
PFEI	=	payload fuel energy intensity, a measure of fuel burn per unit payload per unit range, $\text{kJ}/(\text{kg} \cdot \text{km})$
req_i	=	ith performance requirement for D8 aircraft expressed as an inequality constraint
s_A	=	statistic of interest for random variable $A(\omega)$
s_C	=	statistic of the auxiliary random variable $C(\omega)$
$\hat{s}_A$	=	information-reuse estimator of statistic of interest s_A
$\hat{s}_C$	=	estimator of the statistic of the auxiliary random variable s_C
$\tilde{s}_A$	=	classical control variate estimator of statistic of interest s_A
$\boldsymbol{U}(\omega)$	=	vector of random variables representing the uncertain model parameters
$\boldsymbol{u}$	=	vector of a realization of $\boldsymbol{U}(\omega)$
$\boldsymbol{x}_k$	=	vector of design variables at optimization iteration k
$\boldsymbol{x}_L$, $\boldsymbol{x}_U$	=	lower and upper bounds on design variables, respectively
α, γ	=	parameters in the control variate method
η	=	ratio of estimator variances
λ	=	number of standard deviations from the mean for inequality constraints
ρ_{AC}	=	correlation coefficient between the random variables $A(\omega)$ and $C(\omega)$
$\hat{\rho}_{AC}$, $\hat{\sigma}_A$, $\hat{\gamma}$, $\hat{\eta}$	=	estimators of ρ_{AC}, σ_A, γ, and η, respectively, computed using a_i, c_i for $i = 1, \ldots, n$
σ_A^2, σ_C^2	=	variances of the random variables $A(\omega)$ and $C(\omega)$, respectively

Presented as Paper 2014-0802 at the 10th AIAA Multidisciplinary Design Optimization Conference, National Harbor, MD, 13–17 January 2014; received 16 January 2015; accepted for publication 17 January 2015; published online 26 March 2015.

*Department of Aeronautics and Astronautics.
†Professor, Department of Aeronautics and Astronautics.

I. Introduction

THE D8 aircraft concept was developed at the Massachusetts Institute of Technology, Aurora Flight Sciences, and Pratt and Whitney as part of a NASA-sponsored project to identify enabling technologies and innovative configurations that could allow a subsonic commercial transport aircraft to meet the $N + 3$ goals by the year 2035 [1]. The goals include 70% reduction in fuel burn, 71 dB reduction in effective perceived noise level, and 75% reduction in landing and takeoff NOx emissions relative to the current generation of Boeing 737-800 aircraft. The D8 aircraft concept, rendered in Fig. 1, is in the same class as the Boeing 737-800, carrying 180 passengers over a range of 3000 n mile. The highlights of its features include engines that ingest the fuselage boundary layer, wide lift-generating "double-bubble" fuselage as illustrated in Fig. 2 [2], engine noise shielding by the fuselage and vertical tails, new composite materials, advanced engine thermodynamic cycle, and active load alleviation [1]. Many of these advanced technologies are

Fig. 1 Rendering of the D8 aircraft ([1] Fig. 1).

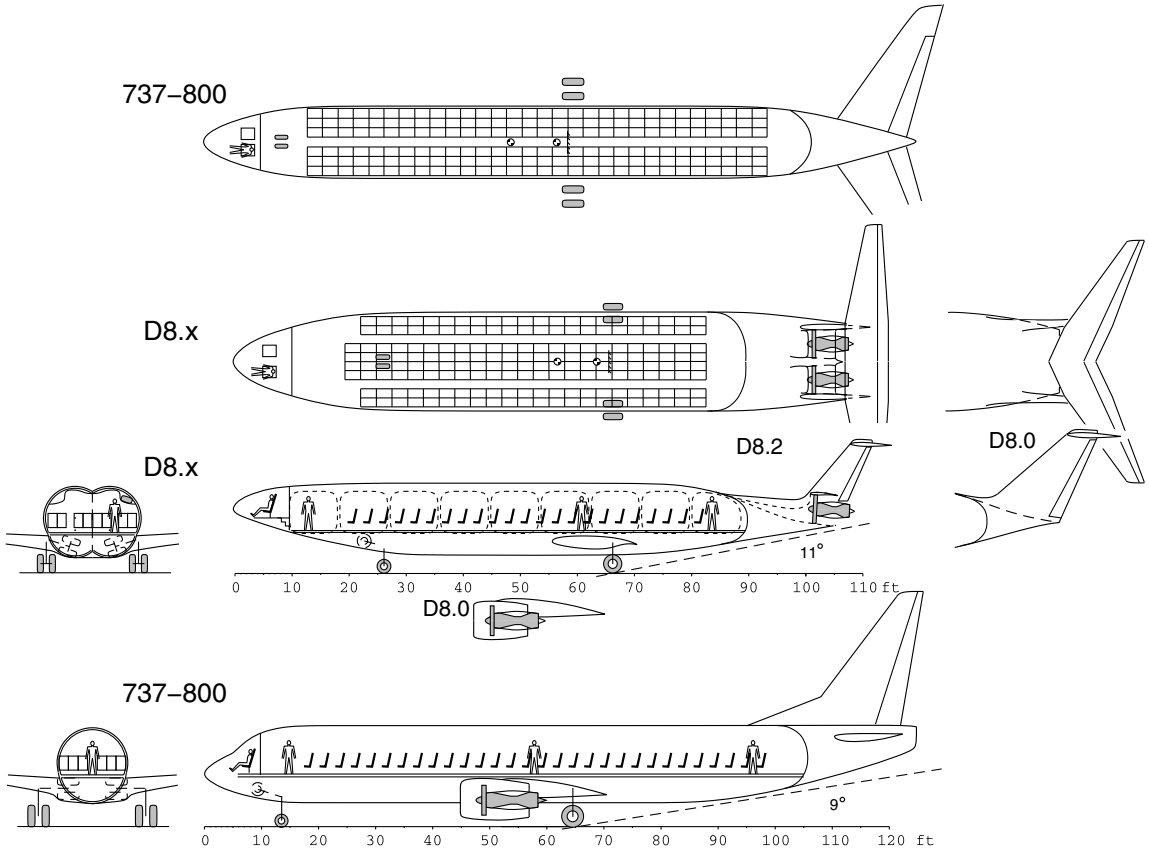

Fig. 2 Comparison of the D8 aircraft and the Boeing 737-800 aircraft ([2] Fig. 22).

still in development, and their expected benefits can only be predicted based on a combination of historical projections, preliminary simulations, and industry expert evaluations. Therefore, there are uncertainties about the effects of each of these technologies that can impact the overall performance of the aircraft. This paper demonstrates an approach developed to account for uncertainties of this kind and hedge against the risks that they represent during the design process. In other words, we optimize the D8 conceptual design to exploit the benefits of the advanced technologies while being insensitive to variations caused by the uncertain future developments of these technologies. The goal is to achieve a robust conceptual aircraft design with minimal need for costly redesigns in the future as the technologies mature over time and their actual benefits are realized.

The approach adopted here to account for uncertainty is based on posing the aircraft design problem as an optimization under uncertainty problem. By accounting for uncertainties in key parameters via rigorous uncertainty analysis, this formulation also has the potential to reassess the conservatism levels of commonly used safety factors and even reconsider the general safety factor approach in the face of emerging technologies. In this formulation, we distinguish between two types of inputs to the problem: design variables, whose values are controlled by the optimizer, and preassigned model parameters, whose values are imposed from the start and not subject to change by the optimizer [3]. In this work, we account for the uncertainties in the imposed values of the model parameters by representing them as random variables with probability distributions based on the best available estimates of the uncertainties in the technologies. Probabilistic treatments of uncertainties in an aerospace design setting have been investigated in the past, using methods such as robust design simulation [4]. Although a probabilistic formulation of the design under uncertainty problem offers flexibility in the quantification of the uncertainties, it can be computationally expensive to solve accurately.

Because the performance metrics of the aircraft (typically outputs of a numerical simulation model) are functions of the design variables and the uncertain model parameters, in our formulation they are also

random variables. We formulate the optimization under uncertainty problem based on the statistics of the performance metrics (e.g., their means and variances). In most cases, the statistic of a performance metric cannot be calculated exactly. Therefore, its value must be approximated numerically. The approximated value is known as the estimator of the statistic, and the approximation error is known as the estimator error. Computing this estimator can be computationally expensive; many evaluations of the numerical simulation model may be required to achieve an acceptably low estimator error. In addition, to solve an optimization under uncertainty problem, the statistics of the performance metrics are needed at many points in the design space. Therefore, the estimators must be computed many times, further exacerbating the computational cost. Reducing the number of model evaluations needed in these computations is critical for wider adoption of optimization under uncertainty during the aircraft design process.

One approach for reducing the computational cost of optimization under uncertainty is to break the nested structure of the problem by introducing surrogate models (e.g., data-fit models) at various levels of the problem formulation [5]. The challenge is in managing the quality of the data-fit models and preventing the optimization routine from exploiting weaknesses in the surrogates [6]. Polynomial-based uncertainty quantification techniques, such as stochastic collocation, can also be applied to the optimization under uncertainty setting by extending the polynomial expansion to include both the design variables and uncertain parameters. However, the increased dimensionality can make it costly to construct the polynomial expansion [7].

In this work, we employ Monte Carlo simulation to estimate the statistics of the aircraft performance metrics because it is applicable to black-box numerical models, scalable to problems with a large number of uncertain parameters, easily parallelizable, numerically robust, and straightforward to implement. Because of the (pseudo) random nature of Monte Carlo sampling, the value of the Monte Carlo estimator is itself also random. The error in the Monte Carlo estimator is characterized by the variance of the estimator. However, the convergence rate of Monte Carlo simulation is slow, and many model evaluations are needed to achieve an acceptably low estimator variance. Ng [8] and Ng and Willcox [9] proposed a multi-information source approach to reduce the computational cost by leveraging approximate sources of information to estimate the statistics of interest. The method is based on the control variate technique for reducing the variance of Monte Carlo estimators by making use of the correlation between the random variable of interest and an auxiliary random variable called the control variate [10,11]. This control variate represents an additional source of information. For example, if the random variable of interest is the aircraft performance metric based on the output of a numerical simulation model at a particular design point, then the control variate could be the output of a lower-fidelity approximation of this numerical simulation model. In this paper, we use the control variate technique to formulate a multi-information source approach to aircraft conceptual design under uncertainty. We consider the particular case where the control variate is defined using the output of the numerical simulation model at a previously evaluated design point; thus, we refer to this new estimator as the "information-reuse estimator."

There have been other recent works on extending the control variate framework to incorporate different kinds of approximate information. The multilevel (or multigrid) Monte Carlo method solves stochastic differential equations by combining multiple levels of coarse discretizations as control variates [12,13]. However, the D8 aircraft optimization under uncertainty problem uses a black-box numerical model that lacks the mathematical structure of stochastic differential equations exploited by the multilevel Monte Carlo method. The reduced-basis control variate Monte Carlo method makes use of control variates that are precomputed offline to reduce the cost of online estimations of the statistics of interest [14,15]. Although our multi-information source approach also makes use of a database of control variates, the database is built-up online during the course of optimization under uncertainty; there are no offline precalculations. Finally, the stacked Monte Carlo method uses supervised learning to create data-fit models as control variates during Monte Carlo simulation [16]. Instead of creating data-fit surrogates, we simply make use of model evaluations at nearby design points, readily available during the course of optimization under uncertainty, as the surrogates.

In this work, we show how our multi-information source approach can be applied in a typical aerospace design setting. Specifically, we show how the information-reuse estimator can be formulated to solve an optimization under uncertainty problem, and we demonstrate that the approach enables practical turnaround time for the D8 aircraft optimization under uncertainty problem. We extend the multi-information source approach to the case of performing trade studies that involve solving multiple optimization under uncertainty problems. Our method leads to computational speedups that contribute an important step toward making a Monte Carlo-based consideration of uncertainties a computationally feasible part of the aircraft conceptual design process.

Section II presents the D8 aircraft optimization under uncertainty example problem. Section III presents the information-reuse estimator and discusses its implementation in the multi-information source approach to solving a general optimization under uncertainty problem. Section IV applies the multi-information source method to the D8 aircraft optimization under uncertainty example problem and demonstrates computational savings relative to the regular Monte Carlo approach. Section V concludes the paper.

II. Problem Setup

The numerical simulation model for this problem is the Transport Aircraft System Optimization (TASOPT) software [17]. It is a multidisciplinary tool for aircraft sizing and mission performance analysis developed for the $N+3$ project with modules in aerodynamics, structural loads and weights, engine cycle analysis, and trajectory simulation. To support the conceptual design of the D8 aircraft with a step change in technology, TASOPT is developed from first principles using low-order physics rather than from empirical or statistical correlations. This allows TASOPT to capture improvements beyond incremental changes from past aircraft that are needed to meet the ambitious $N+3$ goals. This paper considers the optimization of the design of the D8 aircraft subject to randomness in the values of the TASOPT model parameters representing the uncertainties in the advanced technologies.

Given a set of design variables (representing high level geometric, aerodynamic, and engine cycle parameters) and a realization of the uncertain (random) model parameters, TASOPT solves a set of governing equations to generate a feasible aircraft. Other variables such as the detailed sizing and positional parameters of structural members are determined by the governing equations to satisfy internal equality constraints in structural loads, aircraft stability, engine performance, flight trajectory, etc. For example, in the structural module, the skin, stringers, and frames are sized to meet bending and torsion loads on the fuselage. The wing spar is sized to meet the bending moments. The sizes and positions of the primary structure along with those of the secondary components contribute to the overall aircraft weight and moments. The wing area is sized to balance the weight at the given lift coefficient, and the wing position is adjusted to satisfy the stability margin. Similarly, in the engine module, engine cycle analysis is used to size the engine for the start-of-cruise thrust requirement and to determine the weight of fuel needed for the flight profile. For the purpose of the D8 aircraft optimization under uncertainty study, these and other governing equations (see [17] for a full description) are solved simultaneously within TASOPT as a black-box numerical model.

The D8 aircraft mission is to carry 180 passengers over a range of 3000 n mile. The optimization under uncertainty problem considered in this paper has eight design variables ($\boldsymbol{x}$) representing the wing geometry and cruise conditions. Their initial values ($\boldsymbol{x}_0$) and bounds ($\boldsymbol{x}_L$ and $\boldsymbol{x}_U$) are listed in Table 1. Trade studies conducted during the $N+3$ project determined that a slower cruise Mach number of 0.72 is a good balance between lower fuel burn and impacts on airline

Table 1 Initial values, bounds, and optimal values of the D8 aircraft design variables

Variable	Initial value	Lower bound	Upper bound	Case 1 optimum	Case 2 optimum
Cruise lift coefficient	0.71092	0.3	1.0	0.70950	0.69863
Wing aspect ratio	17.07	5	30	16.597	16.476
Wing sweep, deg	17.757	10	30	18.119	18.713
Wing thickness at root	0.13441	0.08	0.20	0.14369	0.14179
Wing thickness at break and tip	0.10079	0.08	0.20	0.10178	0.10198
Wing cruise lift distribution fraction at break	1.136	0.5	1.5	1.1533	1.1429
Wing cruise lift distribution fraction at tip	1.2645	0.5	1.5	1.2981	1.2716
Start of cruise altitude, m	11,784	10,000	13,000	11,793	11,757

operations and passenger experience [1]. Therefore, the cruise Mach number is fixed at 0.72 and is not part of the design space. The design variables in Table 1 are consistent with those used in the conceptual design of the D8 aircraft in the $N + 3$ project except that engine cycle variables including the fan pressure ratio, the bypass ratio, and the turbine inlet temperature are considered fixed. Note that the definition of the conceptual design problem here is not aimed at obtaining comprehensive conceptual design results for the D8 configuration to industry standards. It is constructed to be technically realistic and rich enough to allow both an evaluation of the new proposed approach to design under uncertainty as well as exploratory insights into the nature of the D8 concept design.

The 19 model parameters listed in Table 2 are parameters in the TASOPT low-order physics models whose nominal values for the D8 aircraft were chosen in the $N + 3$ project to reflect the predicted improvements in each of the corresponding technologies. For the optimization under uncertainty problem, we account for the uncertainties in these parameters by representing them as random variables: $\boldsymbol{U}(\omega)$, $\omega \in \Omega$ where Ω is the sample space. The range of values of these uncertain model parameters are obtained from a variety of sources. Ranges for material properties, turbine blade metal temperature, and engine overall pressure ratio are based on the technology maturation roadmap and risk assessment reported in the $N + 3$ project [1,17]. Ranges for the excrescence drag factor are based on Engineering Sciences Data Unit (ESDU) data [18]. Ranges for the engine cooling parameters are based on literature on cooling-flow models [19,20]. Ranges for the remaining parameters are based on best estimates by subject matter experts in the D8 aircraft $N + 3$ team. Given the nominal values and ranges for the uncertain model parameters, we chose triangular distributions with distribution parameters listed in Table 2 to model the uncertainties. Detailed statistical elicitation methods [21] would be another approach to select probability distributions for the uncertain model parameters; this is an area of active research and is beyond the scope of this paper.

Table 2 Triangular distributions of the 19 uncertain model parameters for the D8 aircraft

Random variable	Lower limit	Peak	Upper limit
Vertical load factor for wing bending	2.3	2.5	3.0
Secondary wing components weight fraction	0.49	0.54	0.59
Secondary engine components weight fraction	0.0	0.1	0.2
Material yield stress multiplier	0.8	1.0	1.2
Material density, $\mathrm{lb/in^3}$	0.0504	0.0560	0.0616
Wing excrescence drag factor	1.019	1.025	1.038
Tail excrescence drag factor	1.019	1.025	1.038
Fuselage excrescence drag factor	1.03	1.04	1.08
Fuselage boundary-layer ingestion fraction	0.2	0.4	0.6
Turbine blade metal temperature, K	1450	1500	1550
Turbine cooling Stanton number	0.050	0.065	0.080
Turbine cooling heat transfer efficiency	0.6	0.7	0.8
Turbine cooling film effectiveness factor	0.3	0.4	0.5
Engine overall pressure ratio	45	50	52
Fan efficiency	0.930	0.945	0.950
Low-pressure compressor efficiency	0.89	0.93	0.94
High-pressure compressor efficiency	0.88	0.90	0.93
High-pressure turbine efficiency	0.880	0.925	0.940
Low-pressure turbine efficiency	0.91	0.93	0.95

The design metric is the fuel burn expressed as the payload fuel energy intensity (PFEI): the energy of the fuel used per unit payload and unit range. For the optimization under uncertainty problem, the objective function is defined as the expected fuel burn. As described previously, given the vector of design variables $\boldsymbol{x}$ and a realization $\boldsymbol{u}$ of the uncertain model parameters $\boldsymbol{U}(\omega)$, TASOPT solves the governing equations to satisfy internal constraints for the aircraft. There are four additional performance requirements that are treated externally as inequality constraints for the optimization problem. In the deterministic case, these constraints are (in their nonnormalized form):

$$\mathrm{req}_1(\boldsymbol{x},\boldsymbol{u}) = \text{balanced field length} - 4995\ \text{ft} \le 0 \tag{1a}$$

$$\mathrm{req}_2(\boldsymbol{x},\boldsymbol{u}) = \text{fuel volume} - 90\%\ \text{of internal wing volume} \le 0 \tag{1b}$$

$$\mathrm{req}_3(\boldsymbol{x},\boldsymbol{u}) = \text{span length} - 117.5\ \text{ft} \le 0 \tag{1c}$$

$$\mathrm{req}_4(\boldsymbol{x},\boldsymbol{u}) = 0.015 - \text{top-of-climb gradient} \le 0 \tag{1d}$$

where the top-of-climb gradient is the slope of the flight trajectory at the end of the climb phase.In the presence of randomness where $\boldsymbol{u}$ is a realization of $\boldsymbol{U}(\omega)$, there is a risk that the performance requirements would not be met.[‡] We require that the performance requirements be satisfied for up to λ standard deviation from the mean. Therefore, the D8 aircraft optimization under uncertainty problem is formulated as

$$\begin{aligned}
&\min_{\boldsymbol{x}_L \le \boldsymbol{x} \le \boldsymbol{x}_U} \mathbb{E}[\mathrm{PFEI}(\boldsymbol{x}, \boldsymbol{U}(\omega))] \\
&\text{s.t. } \mathbb{E}[\mathrm{req}_1(\boldsymbol{x}, \boldsymbol{U}(\omega))] + \lambda\sqrt{\mathrm{Var}[\mathrm{req}_1(\boldsymbol{x}, \boldsymbol{U}(\omega))]} \le 0 \\
&\mathbb{E}[\mathrm{req}_2(\boldsymbol{x}, \boldsymbol{U}(\omega))] + \lambda\sqrt{\mathrm{Var}[\mathrm{req}_2(\boldsymbol{x}, \boldsymbol{U}(\omega))]} \le 0 \\
&\mathbb{E}[\mathrm{req}_3(\boldsymbol{x}, \boldsymbol{U}(\omega))] + \lambda\sqrt{\mathrm{Var}[\mathrm{req}_3(\boldsymbol{x}, \boldsymbol{U}(\omega))]} \le 0 \\
&\mathbb{E}[\mathrm{req}_4(\boldsymbol{x}, \boldsymbol{U}(\omega))] + \lambda\sqrt{\mathrm{Var}[\mathrm{req}_4(\boldsymbol{x}, \boldsymbol{U}(\omega))]} \le 0
\end{aligned} \tag{2}$$

[‡]Here, we define the risk as the probability of not satisfying the performance requirements. The risk may be defined in other ways depending on the context and application.

For the numerical results presented in Sec. IV.A, because of the exploratory nature of this work, the value of λ is chosen to be 1. In the case of a normal distribution, this corresponds to 84% probability of satisfying the performance requirements. Sections III.E, IV.B discuss how to trade off the competing goals of reducing the expected fuel burn and reducing the probability of not satisfying the performance requirements.

Note that there are no explicit equality constraints in this optimization problem. The meaning of equality constraints in the presence of uncertainty can be ambiguous. If there are equality constraints, one strategy is to eliminate the equality constraints from the optimization problem and handle them internally in an augmented numerical model (along with the equations of the original numerical model) [8].

To facilitate the presentation of our multi-information source approach in Sec. III, we write the optimization under uncertainty problem in the following general form:

$$\boldsymbol{x}^* = \arg\min_{\boldsymbol{x}} f(\boldsymbol{x}, s_A(\boldsymbol{x})) \quad \text{s.t. } g(\boldsymbol{x}, s_A(\boldsymbol{x})) \le 0 \tag{3}$$

The objective and constraint functions f and g, respectively, depend on the statistic $s_A(\boldsymbol{x})$ (e.g., mean, variance) of the random variable $A(\boldsymbol{x}, \omega)$. Let the numerical model (e.g., TASOPT) be denoted as $M(\boldsymbol{x}, \boldsymbol{u})$, where $\boldsymbol{u}$ is a realization of the uncertain model parameters $\boldsymbol{U}(\omega)$. Then, the random variable $A(\boldsymbol{x}, \omega) = M(\boldsymbol{x}, \boldsymbol{U}(\omega))$ is the output of the model (here PFEI, balanced field length, span length, etc.). Because $s_A(\boldsymbol{x})$ cannot be evaluated analytically in most cases, we compute an estimator $\hat{s}_A(\boldsymbol{x})$ (i.e., a numerical approximation of s_A) to a specified root mean square error (RMSE). Therefore, the objective and constraints in Eq. (3) are estimated as $\hat{f}(\boldsymbol{x}) = f(\boldsymbol{x}, \hat{s}_A(\boldsymbol{x}))$ and $\hat{g}(\boldsymbol{x}) = g(\boldsymbol{x}, \hat{s}_A(\boldsymbol{x}))$.

The discussion of the results in Sec. IV will return to the D8 aircraft optimization under uncertainty problem in Eq. (2).

III. Multi-Information Source Approach

Solving the general optimization under uncertainty problem in Eq. (3) can be computationally expensive; at every step in the design space toward the optimum, $\boldsymbol{x}_k, k = 0, 1, 2, \ldots$, we need to calculate the estimator $\hat{s}_A(\boldsymbol{x}_k)$. This work focuses on Monte Carlo simulation because it is nonintrusive and parallelizable, and convergence is independent of the dimension of the uncertain model parameters. However, it may require many expensive model evaluations to achieve an acceptably low estimator RMSE. We reduce the computational cost by making use of the control variate method to leverage the model autocorrelation in the design space, that is, the correlation between $M(\boldsymbol{x}, \boldsymbol{U}(\omega))$ and $M(\boldsymbol{x} + \Delta\boldsymbol{x}, \boldsymbol{U}(\omega))$ for small $\Delta\boldsymbol{x}$. This section begins with a discussion on the basic Monte Carlo approach.

A. Monte Carlo Simulation

Consider estimating $s_A = \mathbb{E}[A(\omega)]$ of a random variable $A(\omega)$. Given n independent and identically distributed samples $a_1, a_2, \ldots, a_n$ drawn from the distribution of $A(\omega)$, the regular Monte Carlo estimator of s_A, denoted as $\bar{a}_n$, is

$$\bar{a}_n = \frac{1}{n}\sum_{i=1}^{n} a_i \tag{4}$$

Its mean square error (MSE) is obtained by computing the estimator variance

$$\mathrm{MSE}[\bar{a}_n] = \mathrm{Var}[\bar{a}_n] = \frac{1}{n^2}\mathrm{Var}\left[\sum_{i=1}^{n} a_i\right] = \frac{\sigma_A^2}{n} \tag{5}$$

where $\sigma_A^2 = \mathrm{Var}[A(\omega)]$ is the variance of the random variable $A(\omega)$. Our approach to reducing the number of samples needed to achieve an acceptably low estimator variance (i.e., estimator MSE) is based on the control variate method [10,11], which makes use of the correlation between the random variable $A(\omega)$ and an auxiliary random variable $C(\omega)$.

The optimization under uncertainty problem in Eq. (3) requires estimation of the statistics of the output of the numerical model $M(\boldsymbol{x}_k, \boldsymbol{U}(\omega))$ at a particular vector of design variables $\boldsymbol{x}_k$. For estimating the mean of the model output, the Monte Carlo samples are thus defined as

$$a_i = M(\boldsymbol{x}_k, \boldsymbol{u}_i), \qquad i = 1, \ldots, n \tag{6}$$

where $\boldsymbol{u}_i$ are independent and identically distributed samples drawn from the distribution of the uncertain model parameters $\boldsymbol{U}(\omega)$. From the previous Monte Carlo framework, we have

$$\bar{a}_n = \frac{1}{n}\sum_{i=1}^{n} a_i = \frac{1}{n}\sum_{i=1}^{n} M(\boldsymbol{x}_k, \boldsymbol{u}_i) \tag{7}$$

To apply the same control variate framework for estimating the variance of the model output, we define the Monte Carlo samples as

$$b_i = \frac{n}{n-1}\left(M(\boldsymbol{x}_k, \boldsymbol{u}_i) - \frac{1}{n}\sum_{j=1}^{n} M(\boldsymbol{x}_k, \boldsymbol{u}_j)\right)\left(M(\boldsymbol{x}_k, \boldsymbol{u}_i) - \frac{1}{n-1}\sum_{j=1}^{n-1} M(\boldsymbol{x}_k, \boldsymbol{u}_j)\right), \qquad i = 1, \ldots, n \tag{8}$$

That is, the samples are residuals based on the one-pass algorithm for computing the variance [22]. From the same Monte Carlo framework, we have

$$\bar{b}_n = \frac{1}{n}\sum_{i=1}^{n} b_i = \frac{1}{n-1}\sum_{i=1}^{n}\left(M(\boldsymbol{x}_k, \boldsymbol{u}_i) - \frac{1}{n}\sum_{j=1}^{n} M(\boldsymbol{x}_k, \boldsymbol{u}_j)\right)^2 \tag{9}$$

Therefore, the discussion in subsequent sections will assume that we are estimating the mean of the model output with the understanding that the same approach can be applied to estimate the variance of the model output by redefining the Monte Carlo samples as described previously.

After computing the estimator $\hat{s}_A$ at $\boldsymbol{x}_k$, we evaluate the objective and constraint functions. Typically, we are interested in the error of $\hat{f}$ and $\hat{g}$ rather than the error in $\hat{s}_A$ directly. By taking a first-order Taylor expansion of the function f (and similarly for g) about the statistic s_A and then taking the expectation, the error of the objective and constraint functions is related to the estimator variance by

$$\mathrm{MSE}[\hat{f}(\boldsymbol{x}_k)] \approx \nabla_s f(\boldsymbol{x}_k, \hat{s}_A)^T \,\mathrm{Var}[\hat{s}_A] \nabla_s f(\boldsymbol{x}_k, \hat{s}_A) \tag{10}$$

where $\nabla_s f(\boldsymbol{x}_k, \hat{s}_A)$ is the gradient of f with respect to the statistic s_A, and $\mathrm{Var}[\hat{s}_A]$ is the estimator variance.

B. Control Variate Method

Computing the regular Monte Carlo estimator can be computationally expensive because it has a relatively slow error convergence rate of $n^{1/2}$, where n is the number of samples used. The control variate method [10,11] is an estimator variance reduction technique; it reduces the constant factor of the error convergence. Although the convergence rate does not change, it has the effect of shifting the convergence curve downward. For a given desired error level, this downward shift can result in relatively large computational savings because of the shallow convergence curve.

The control variate method reduces the estimator variance by using an auxiliary random variable $C(\omega)$, known as the control variate, to make a correction to the regular Monte Carlo estimator of $s_A = \mathbb{E}[A(\omega)]$. The control variate estimator is

$$\hat{s}_A = \bar{a}_n + \alpha(s_C - \bar{c}_n) \tag{11}$$

where $\bar{a}_n$ and $\bar{c}_n$ are the regular Monte Carlo estimators of $A(\omega)$ and $C(\omega)$, respectively, using n samples, and α is the control variate

parameter to be determined. In the classical control variate method, it is assumed that the exact mean of the auxiliary random variable, $s_C = \mathbb{E}[C(\omega)]$, is known. The correction applied to $\bar{a}_n$ does not change the expectation of the estimator, but it does add additional terms to the estimator variance:

$$\mathrm{Var}[\tilde{s}_A] = \frac{1}{n}(\sigma_A^2 + \alpha^2\sigma_C^2 - 2\alpha\rho_{AC}\sigma_A\sigma_C) \tag{12}$$

where $\sigma_C^2 = \mathrm{Var}[C(\omega)]$ is the variance of the auxiliary random variable $C(\omega)$, and $\rho_{AC} = \mathrm{Corr}[A(\omega), C(\omega)]$ is the correlation coefficient between the two random variables.

The control variate parameter α is determined by minimizing the estimator variance for a given fixed number of samples n. This results in

$$\alpha = \rho_{AC}\frac{\sigma_A}{\sigma_C} \tag{13}$$

and

$$\mathrm{MSE}[\tilde{s}_A] = \mathrm{Var}[\tilde{s}_A] = (1 - \rho_{AC}^2)\frac{\sigma_A^2}{n} \tag{14}$$

Comparing Eq. (14) with Eq. (5) reveals that the control variate estimator is effective at reducing the estimator variance when the random variable $A(\omega)$ and the auxiliary random variable $C(\omega)$ are correlated. In fact, the factor $(1 - \rho_{AC}^2)$ in Eq. (14) is guaranteed to be less than or equal to 1. In essence, the control variate estimator incorporates information about the auxiliary random variable to reduce the estimator error. This can be interpreted from a regression point of view. Figure 3 illustrates a scatter plot of n samples of $A(\omega)$ and $C(\omega)$ and the linear regression of the samples with slope α. The values of the regular Monte Carlo estimators $\bar{a}_n$ and $\bar{c}_n$ can be computed from these samples as defined in Eq. (4). Given $s_C = \mathbb{E}[C(\omega)]$, the control variate method makes an adjustment to $\bar{a}_n$ based on the difference $s_C - \bar{c}_n$ and the slope of the regression line α to obtain the control variate estimator $\tilde{s}_A$. We make use of this framework for the information-reuse estimator next to leverage information from previous optimization iterations.

C. Information-Reuse Estimator

To solve the general optimization under uncertainty problem in Eq. (3), the statistics of the model have to be estimated at a sequence of vectors of design variables $\{\boldsymbol{x}_0, \boldsymbol{x}_1, \ldots, \boldsymbol{x}_k\}$ determined by the optimization routine as it progresses toward the optimal design. At the current optimization iteration k, we define the random variable $A(\omega) = M(\boldsymbol{x}_k, \boldsymbol{U}(\omega))$, and we wish to compute an estimator $\hat{s}_A$ of the statistic $s_A = \mathbb{E}[A(\omega)]$. The control variate method makes use of a correlated auxiliary random variable $C(\omega)$. Here, a good candidate for $C(\omega)$ is $M(\boldsymbol{x}_k + \Delta\boldsymbol{x}, \boldsymbol{U}(\omega))$ for small $\Delta\boldsymbol{x}$. It can be shown that, if the model is twice differentiable in the design space, then the correlation coefficient between $M(\boldsymbol{x}_k, \boldsymbol{U}(\omega))$ and $M(\boldsymbol{x}_k + \Delta\boldsymbol{x}, \boldsymbol{U}(\omega))$ approaches 1 quadratically as $\Delta\boldsymbol{x} \to 0$ [8]. Therefore, we define the auxiliary random variable to be the model evaluated at the closest previous design point, $C(\omega) = M(\boldsymbol{x}_{\ell}, \boldsymbol{U}(\omega))$, where

$$\ell = \underset{\ell' < k}{\arg\min} \|\boldsymbol{x}_k - \boldsymbol{x}_{\ell'}\| \tag{15}$$

The classical control variate method requires the exact mean of the auxiliary random variable, $s_C = \mathbb{E}[C(\omega)]$, which is unknown in this context. Instead, we replace s_C with the estimator computed during the previous optimization iteration ℓ and denote it as $\hat{s}_C$. We assume that all previously computed estimators and their variances from past optimization iterations have been stored in a database and are available for retrieval during the current optimization iteration k. The information-reuse estimator is adapted from the classical control variate method as follows:

$$\hat{s}_A = \bar{a}_n + \gamma(\hat{s}_C - \bar{c}_n) \tag{16}$$

The expectation of the information-reuse estimator is

$$\begin{aligned}\mathbb{E}[\hat{s}_A] &= \mathbb{E}[\bar{a}_n] + \gamma(\mathbb{E}[\hat{s}_C] - \mathbb{E}[\bar{c}_n]) \\ &= \mathbb{E}[A(\omega)] + \gamma(\mathbb{E}[C(\omega)] - \mathbb{E}[C(\omega)]) = \mathbb{E}[A(\omega)]\end{aligned} \tag{17}$$

and the variance of the information-reuse estimator is

$$\begin{aligned}\mathrm{Var}[\hat{s}_A] &= \mathrm{Var}[\bar{a}_n] + \gamma^2(\mathrm{Var}[\hat{s}_C] + \mathrm{Var}[\bar{c}_n]) - 2\gamma\,\mathrm{Cov}[\bar{a}_n, \bar{c}_n] \\ &= \frac{\sigma_A^2}{n} + \gamma^2\left(\mathrm{Var}[\hat{s}_C] + \frac{\sigma_C^2}{n}\right) - 2\gamma\frac{\rho_{AC}\sigma_A\sigma_C}{n} \\ &= \frac{1}{n}[\sigma_A^2 + \gamma^2\sigma_C^2(1+\eta) - 2\gamma\rho_{AC}\sigma_A\sigma_C]\end{aligned} \tag{18}$$

where

$$\eta = \frac{\mathrm{Var}[\hat{s}_C]}{\mathrm{Var}[\bar{c}_n]} = \frac{\mathrm{Var}[\hat{s}_C]}{\sigma_C^2/n} \tag{19}$$

The estimator variance is derived assuming that $\hat{s}_C$, the information-reuse estimator computed during optimization iteration ℓ, is uncorrelated with $\bar{a}_n$ or $\bar{c}_n$, which are computed at the current optimization iteration k. In other words, we require that $\mathrm{Cov}[\hat{s}_C, \bar{a}_n] = \mathrm{Cov}[\hat{s}_C, \bar{c}_n] = 0$. To achieve this, the set of realizations of the uncertain model parameters $\boldsymbol{U}(\omega)$ used in optimization iteration k must be independent of the set of realizations of $\boldsymbol{U}(\omega)$ used in optimization iteration ℓ.

Given a fixed number of samples n, the information-reuse estimator variance is minimized by the following choice of the control variate parameter:

$$\gamma = \left(\frac{\rho_{AC}}{1+\eta}\right)\frac{\sigma_A}{\sigma_C} \tag{20}$$

resulting in the information-reuse estimator variance

$$\mathrm{Var}[\hat{s}_A] = \left(1 - \frac{\rho_{AC}^2}{1+\eta}\right)\frac{\sigma_A^2}{n} \tag{21}$$

A reduction in the error of the information-reuse estimator relative to the regular Monte Carlo estimator using n samples is achieved when the correlation coefficient ρ_{AC} is close to 1 (or -1).

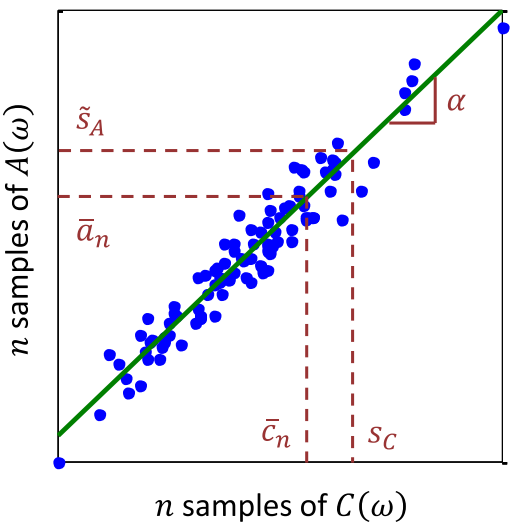

Fig. 3 Illustration of the regression interpretation of the control variate method. The dots are samples of the random variables $A(\omega)$ and $C(\omega)$.

At the current optimization iteration k, independent and identically distributed samples $\boldsymbol{u}_i$, $i = 1, 2, 3, \ldots, n$ are drawn from the distribution of $\boldsymbol{U}(\omega)$, and the model is evaluated at both $\boldsymbol{x}_k$ and $\boldsymbol{x}_\ell$ per sample to compute $\bar{a}_n$ and $\bar{c}_n$. In terms of the number of the model evaluations, the computational effort for the regular Monte Carlo estimator $\bar{a}_n$ is n, whereas the computational effort for the information-reuse estimator $\hat{s}_A$ is $2n$. Let $p = 2n$ denote the computational effort for the information-reuse estimator. The MSE of the information-reuse estimator in terms of its computational effort is

$$\mathrm{MSE}[\hat{s}_{A,p}] = \mathrm{Var}[\hat{s}_{A,p}] = 2\left(1 - \frac{\rho_{AC}^2}{1+\eta}\right)\frac{\sigma_A^2}{p} \tag{22}$$

Unlike the classical control variate method, the factor $2(1 - \rho_{AC}^2/1 + \eta)$ in Eq. (22) is not guaranteed to be less than or equal to 1. Therefore, if the correlation coefficient ρ_{AC} is not high enough (e.g., when $\boldsymbol{x}_\ell$ is far from $\boldsymbol{x}_k$), the information-reuse estimator may require more computational effort to achieve the same MSE as the regular Monte Carlo estimator. If we detect this situation, say, by comparing Eqs. (5) and (22), we switch back to the regular Monte Carlo estimator for this optimization iteration as a safeguard.

D. Implementation

The implementation of our approach is illustrated by the flowcharts in Figs. 4 and 5. Figure 4 describes the "outer loop" in which an optimization routine iterates to search the design space for the optimum. Figure 5 describes the "inner loop" to calculate the information-reuse estimator at the design point of every optimization iteration.

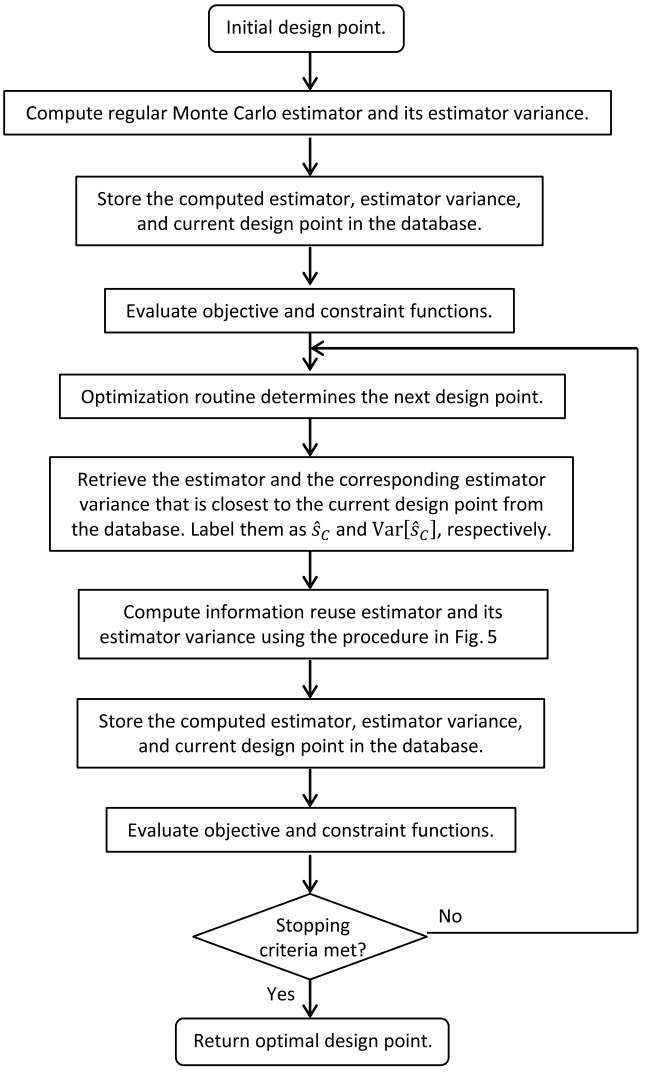

Fig. 4 Flowchart illustrating the outer loop of the multi-information source approach for optimization under uncertainty.

Let us consider an optimization algorithm that generates a sequence of design points $\boldsymbol{x}_k$, $k = 0, 1, 2, \ldots$, in its search for the optimal design. At each optimization iteration k, we choose a past optimization iteration $\ell = \arg\min_{\ell' < k} \|\boldsymbol{x}_k - \boldsymbol{x}_{\ell'}\|$ and retrieve from the database $\boldsymbol{x}_\ell$ and the corresponding estimator $\hat{s}_C$ and estimator variance $\mathrm{Var}[\hat{s}_C]$.

Next, we step into the inner loop described by Fig. 5 to compute the estimator at $\boldsymbol{x}_k$. As described at the end of Sec. III.C, we need to determine whether to use the information-reuse estimator or to fall back to the regular Monte Carlo estimator. Therefore, we start by drawing an initial number of samples $\{\boldsymbol{u}_i\}_{i=1}^n$, $n = n_{\mathrm{init}}$, from the distribution of $\boldsymbol{U}(\omega)$ and evaluate $M(\boldsymbol{x}_k, \boldsymbol{u}_i)$ and $M(\boldsymbol{x}_\ell, \boldsymbol{u}_i)$ to generate the pairs of samples $\{a_i, c_i\}_{i=1}^n$. We calculate the number of model evaluations needed to meet the desired MSE for the regular Monte Carlo estimator from Eq. (5) and the corresponding number needed for the information-reuse estimator from Eq. (22). If the regular Monte Carlo estimator would require more model evaluations, we continue with the information-reuse estimator. Otherwise, we continue with the regular Monte Carlo estimator instead. This latter outcome would happen if the samples at design points $\boldsymbol{x}_k$ and $\boldsymbol{x}_\ell$ were not sufficiently correlated.

If we continue with the information-reuse estimator, we increase n and generate additional pairs of samples of a_i and c_i. We compute the information-reuse estimator $\hat{s}_{A,p}$ and its estimator variance $\mathrm{Var}[\hat{s}_{A,p}]$ from Eqs. (16, 22), respectively. However, the values of σ_A, σ_C, and ρ_{AC} are unknown. Therefore, following the approach taken in the classical control variate method, we replace them with their sample estimates from the samples $\{a_i, c_i\}_{i=1}^n$:

$$\hat{\rho}_{AC}^2 = \frac{[\sum_{i=1}^n (a_i - \bar{a}_n)(c_i - \bar{c}_n)]^2}{[\sum_{i=1}^n (a_i - \bar{a}_n)^2][\sum_{i=1}^n (c_i - \bar{c}_n)^2]} \tag{23}$$

$$\hat{\sigma}_A^2 = \frac{\sum_{i=1}^n (a_i - \bar{a}_n)^2}{n-1} \tag{24}$$

$$\hat{\gamma} = \frac{1}{1+\hat{\eta}} \frac{\sum_{i=1}^n (a_i - \bar{a}_n)(c_i - \bar{c}_n)}{\sum_{i=1}^n (c_i - \bar{c}_n)^2} \tag{25}$$

$$\hat{\eta} = \frac{\mathrm{Var}[\hat{s}_C] n(n-1)}{\sum_{i=1}^n (c_i - \bar{c}_n)^2} \tag{26}$$

If the MSE (i.e., $\mathrm{Var}[\hat{s}_{A,p}]$) is unacceptable, we increase n and compute the information-reuse estimator and its estimator variance again.

If the MSE is acceptable, we return to the outer loop described by Fig. 4. We evaluate the objective and constraint functions $\hat{f}(\boldsymbol{x}_k) = f(\boldsymbol{x}_k, \hat{s}_{A,p})$ and $\hat{g}(\boldsymbol{x}_k) = g(\boldsymbol{x}_k, \hat{s}_{A,p})$. Before the end of optimization iteration k, we store $\hat{s}_{A,p}$ and $\mathrm{Var}[\hat{s}_{A,p}]$ in the database to provide candidates for $\hat{s}_C$ and $\mathrm{Var}[\hat{s}_C]$ for subsequent optimization iterations. Finally, we return the values $\hat{f}(\boldsymbol{x}_k)$ and $\hat{g}(\boldsymbol{x}_k)$ to the optimization routine to determine the next design point $\boldsymbol{x}_{k+1}$ for optimization iteration $k+1$ and repeat.

Note that, at the initial design point $\boldsymbol{x}_0$, we cannot compute the information-reuse estimator because the database is empty. Therefore, we start with the regular Monte Carlo estimator at the initial design point. This means that the first optimization iteration tends to be the most computationally expensive. However, as the optimization progresses, the database of candidates for $\hat{s}_C$ and $\mathrm{Var}[\hat{s}_C]$ grows. Furthermore, typical optimization algorithms take shorter and shorter steps as they approach the optimum, reducing $\|\boldsymbol{x}_k - \boldsymbol{x}_\ell\|$ and potentially improving the approximation

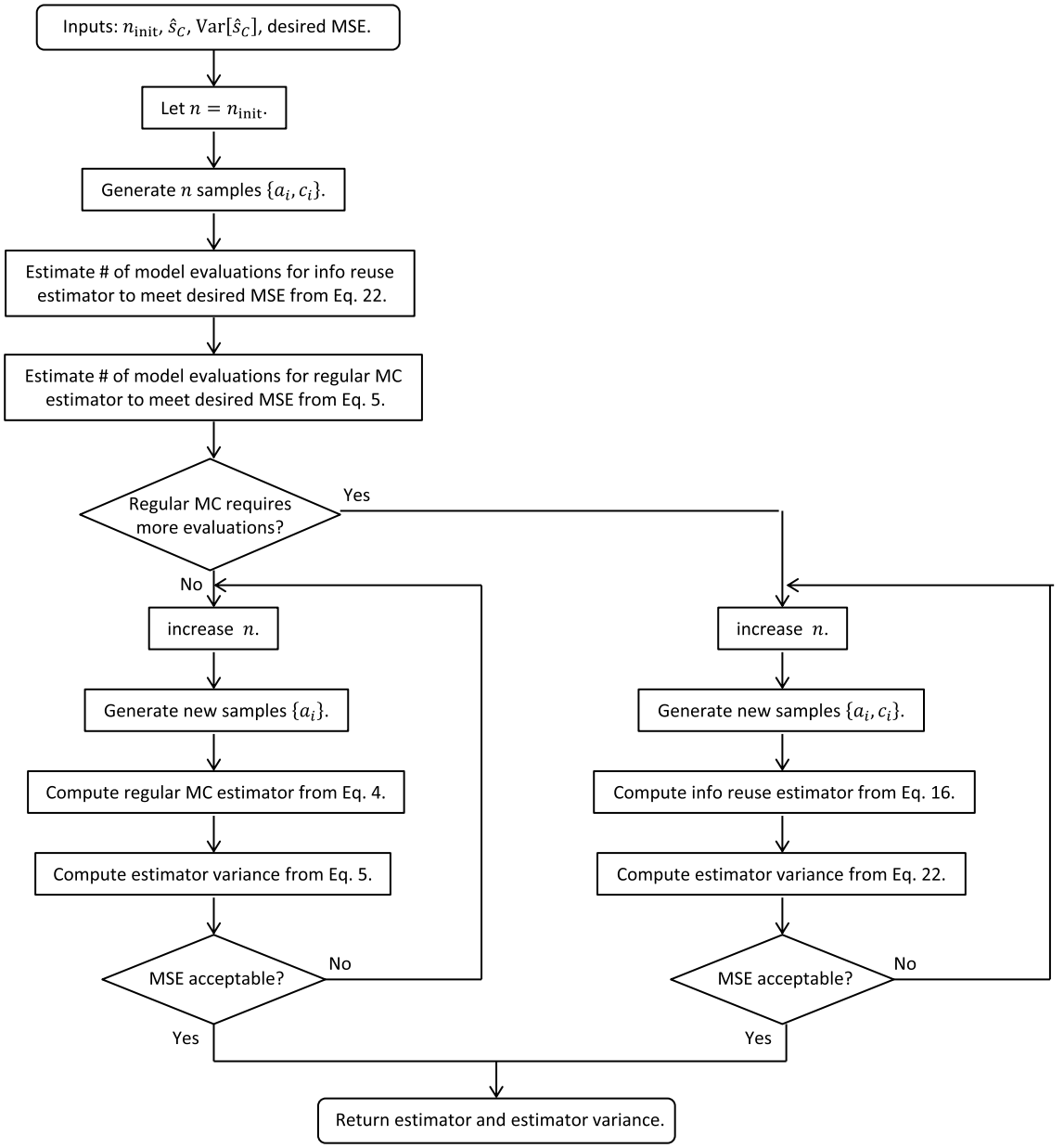

Fig. 5 Flowchart illustrating the procedure to compute the information-reuse estimator (info reuse) with fallback to the regular Monte Carlo estimator (regular MC).

$M(\boldsymbol{x}_\ell, \boldsymbol{U}(\omega))$ of $M(\boldsymbol{x}_k, \boldsymbol{U}(\omega))$. This makes the information-reuse estimator increasingly effective as the optimization progresses.

E. Pareto Frontier Exploration and Trade Studies

When there are multiple objectives of interest in an optimization problem, it is often informative to generate the Pareto frontier and study the tradeoff between the competing objectives. A Pareto frontier is the set of optimal designs in which it is impossible to improve one objective without worsening another objective. Methods to determine the Pareto frontier include the weighted sum, the adaptive weighted sum [23], and the normal boundary intersection [24]. They require solving a sequence of optimization problems to search for the points along the Pareto frontier.

Many optimization under uncertainty problems have competing goals of minimizing the expected cost and the risk. For example, it would be worthwhile in Eq. (2) to adjust the weight λ and study the tradeoff between the expected fuel burn and the risk of not satisfying the performance criteria. Generating a Pareto frontier in this case (using methods such as the weighted sum) would require solving a sequence of optimization under uncertainty problems, each with a different value of λ, which can be computationally expensive even with the savings provided by the information-reuse estimator. Fortunately, because the same statistics of the model output (e.g., mean and variance) are calculated for each optimization under uncertainty problem in the sequence, then, using our multi-information source approach, each problem need not be solved from scratch.

As discussed previously, the first few optimization iterations using the information-reuse estimator require the most computational effort because the database of past optimization iterations has yet to be built up. To reduce this computational cost, we reuse the database of estimators from the previous optimization under uncertainty problem in the next optimization under uncertainty problem. This is possible because the same statistics are being estimated at the design points visited by each optimization under uncertainty problem in the sequence; the only difference between the problems is the objective and/or constraint functions of those statistics. Reusing the database means that there are good candidates for the auxiliary random variable starting from the first optimization iteration (except for the

first iteration of the first optimization under uncertainty problem), and therefore the information-reuse estimator requires relatively little computational effort even at the start of each optimization under uncertainty problem.

IV. Numerical Results

The optimization under uncertainty problem of interest as an example here is the conceptual design of the D8 aircraft. We solve Eq. (2) using both the regular Monte Carlo estimator and the information-reuse estimator to compare their computational costs. We also demonstrate how our multi-information source approach can be used to study the risk–performance tradeoff that requires solving many optimization under uncertainty problems.

A. Comparison of Computational Costs

We consider two cases: at each optimization iteration, the objective and constraint functions are evaluated using 1) the regular Monte Carlo estimator, and 2) the information-reuse estimator. In both cases, the tolerance on the root mean square error (RMSE) of the objective function estimator is fixed at 1×10^{-3}, whereas the tolerance on the RMSE of the constraint function estimators is fixed at 5×10^{-4} for all optimization iterations. The initial number of samples n_{init} is 32. Because of the pseudorandomness of Monte Carlo sampling, the objective and constraint values returned to the optimization routine are noisy, which poses a challenge for any optimization routine that is not noise-tolerant. We employ the COBYLA derivative-free constrained optimization routine [25] to solve the D8 aircraft optimization under uncertainty problem in Eq. (2). It constructs linear interpolation models of the objective and constraint functions using evaluations on a simplex in the design space. New vectors of design variables are obtained either by solving a linear programming subproblem using the interpolation models or by improving the geometry of the simplex. Although derivative-free routines such as COBYLA are not developed specifically for noisy optimization problems, they are typically tolerant to small levels of noise in practice [26].

The convergence of the objective (expected fuel burn) as a function of the cumulative computational effort is shown in Fig. 6, where the computational effort is the number of TASOPT model evaluations. In total, case 1 required 1.13×10^6 model evaluations, and case 2 required 1.16×10^5 model evaluations. Thus, the multi-information source approach using the information-reuse estimator provided about 90% savings in computational effort over using the regular Monte Carlo estimator. Each evaluation of TASOPT takes about 0.5 s on a desktop computer.[§] When evaluating the model in parallel on four cores, the D8 aircraft optimization under uncertainty problem was solved in 237 min with the information-reuse estimator compared to 38 h with the regular Monte Carlo estimator. Although we have used four cores here, as a sampling-based method the information-reuse estimator can be easily parallelized to use more cores if the computational resources are available.

Figure 7 plots the computational effort required to compute the estimators in case 1 and case 2 at each optimization iteration. After the first few optimization iterations, the information-reuse estimator requires significantly less computational effort than the regular Monte Carlo estimator to achieve the required RMSE tolerance because the database of past optimization iterations has built up sufficiently to provide good candidates for the auxiliary random variable. Many optimization iterations after iteration 20 only needed the minimal number of sample points ($n_{\text{init}} = 32$, corresponding to computational effort of 64) to meet the desired RMSE. As described in Fig. 5, at least n_{init} samples are generated at each optimization iteration to decide whether to continue with the information-reuse estimator or to fall back to the regular Monte Carlo estimator. Overall, in case 2, only 10 out of 41 optimization iterations had to fall back to the regular Monte Carlo estimator, and they occur mostly during the first few optimization iterations.

[§]The computer processor is an Intel Core i7-2600 with four cores at 3.4 GHz.

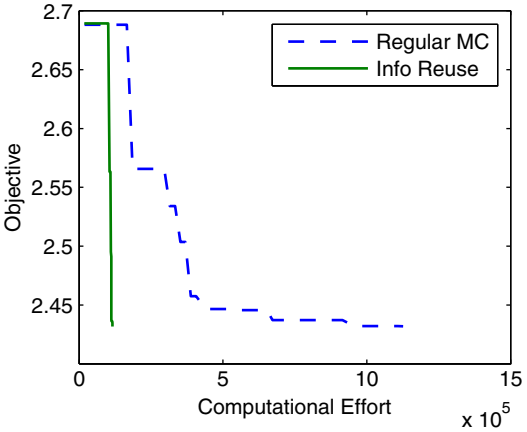

Fig. 6 Comparison of convergence histories for the D8 aircraft optimization under uncertainty problem using 1) the regular Monte Carlo estimator (regular MC), and 2) the information-reuse estimator (info reuse).

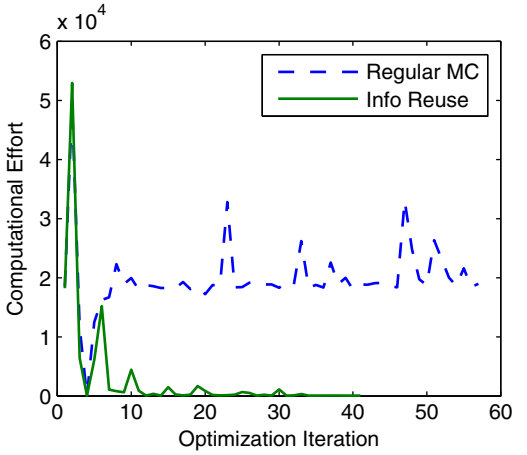

Fig. 7 Computational effort in terms of the number of model evaluations per optimization iteration.

The correlation coefficient $\hat{\rho}_{AC}$ for the expected fuel burn used to compute the information-reuse estimator at each optimization iteration is shown in Fig. 8a. It can be seen that the correlation coefficient is close to one for the later optimization iterations. As mentioned previously, this is partly a result of the database being built up at the optimization progresses, but it is also a result of the optimization routine taking smaller and smaller steps as it refines the location of the optimum (see Fig. 8b). As discussed in Sec. III.C, the model at a previous design point is a good approximation of the model at the current design point when the distance between the design points are small. The regular Monte Carlo estimator discards this information and computes a new estimator independently at each optimization iteration. On the other hand, our multi-information source approach using the information-reuse estimator captures this information in the database and makes use of it by means of the correlation coefficient.

By optimizing the aircraft design while taking into account the uncertainties of the technological projections, the expected fuel burn decreased from 2.69 to 2.43 kJ/(kg · km). The optimal aircraft design has an 84% chance of satisfying the performance requirements compared to a 22% chance for the initial aircraft design, with the two critical constraints being the balanced field length requirement and the span length requirement. The optimal design variables found using the regular Monte Carlo estimator and those found using the information-reuse estimator are listed in Table 1. In both cases, the most significant change is the decease in wing aspect

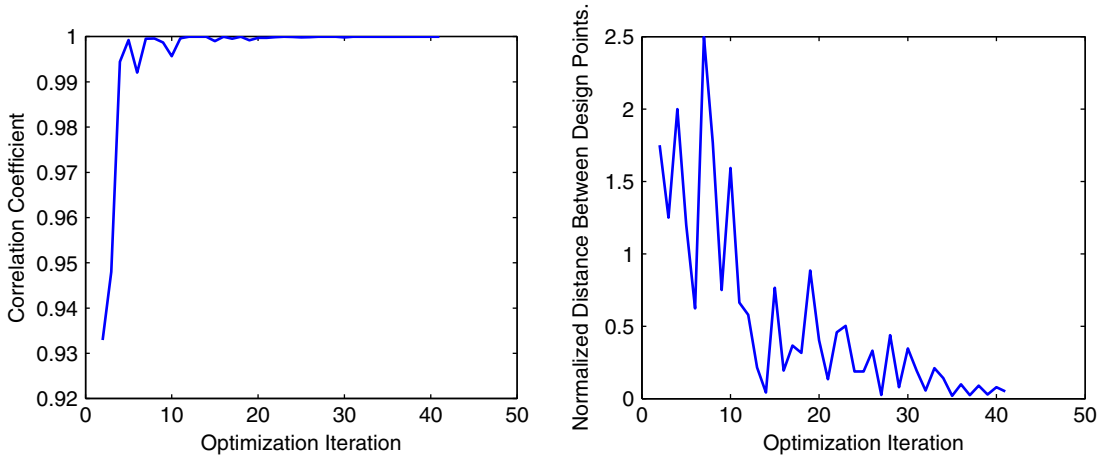

a) Correlation coefficient $\hat{\rho}_{AC}$ b) Normalized distance $\|\mathbf{x}_k - \mathbf{x}_\ell\|$

Fig. 8 Correlation coefficient and the normalized distance between the design point at the current optimization iteration and the design point at the past optimization iteration.

ratio so that the wing area can increase by about 3% without increasing the span length. There is a corresponding increase in the wing thickness at the wing root to support the increased wing area.

B. Risk–Performance Tradeoff Studies

In Sec. II, λ is set to one for the constraints of the D8 concept aircraft optimization under uncertainty problem. However, the value $\lambda = 1$ is chosen somewhat arbitrarily as a balance between performance, defined as the expected fuel burn of the optimal aircraft, and design risk, defined as the probability of not satisfying the performance requirements. Therefore, it is useful to investigate the tradeoff between the performance and the risk. For simplicity, rather than applying methods such as the adaptive weighted sum or the normal boundary intersection mentioned in Sec. III.E to generate a sequence of optimization under uncertainty problems to solve, we vary λ in equal steps from 0 to 3 and resolve the optimization under uncertainty problem for each value of λ to produce the Pareto frontier. As discussed in Sec. III.E, because the only difference between each optimization under uncertainty problem is the value of λ, we reuse the database of past optimization iterations in the sequence of optimization under uncertainty problems to reduce the computational cost. This has the effect of further reducing the computational effort of the information-reuse estimator, especially during the first few optimization iterations of each optimization under uncertainty problem.

The Pareto frontier for the D8 concept aircraft is plotted in Fig. 9a. We see that, although it is necessary to sacrifice expected fuel burn to reduce the risk of not satisfying the performance requirements, the increase in expected fuel burn is not large, demonstrating that the D8 aircraft concept design is relatively insensitive to the uncertainties. Figure 9b shows the trend in the wing aspect ratio along the Pareto frontier. It can be seen that the reduction in the wing aspect ratio is a major driver for the increase in expected fuel burn; other design variables do not show such a clear trend. If we first solve the deterministic optimization problem with the 19 uncertain model parameters fixed at the peak of the triangular distributions and then reintroduce the uncertainties to the parameters to compute the statistics of the deterministic optimal design, the mean fuel burn is 0.999 on the relative scale in Fig. 9a, but the probability of satisfying the performance requirements is only about 30%. This demonstrates that uncertainties must be taken into account during the design process, not afterward.

As a comparison, we investigate the effect of the airframe size and configuration on the aircraft's sensitivity to the uncertainties. We consider a hypothetical advanced-technology 737 aircraft, which is in the same class as the D8 concept aircraft with 180 passengers and 3000 n mile range. We define this hypothetical aircraft to be outfitted with the same advanced technologies as the D8 concept aircraft, except that it has a conventional fuselage and two engines under the wings (see the 737 schematic in Fig. 2). Therefore, it has the same uncertain model parameters as those listed in Table 2 for the D8 concept aircraft; however, the fuselage boundary-layer ingestion fraction parameter is not included because it is not applicable to the conventional airframe configuration. The optimization under uncertainty problem formulation for the advanced-technology 737

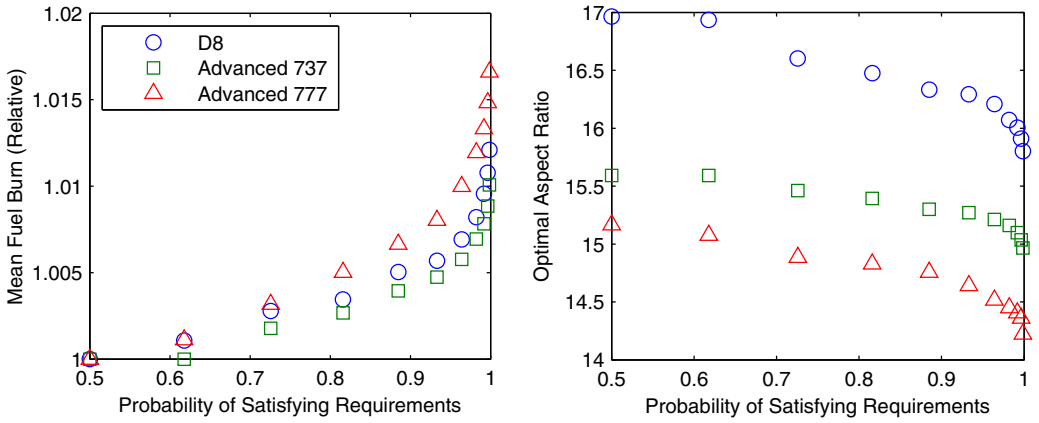

a) Pareto frontiers b) Trends of the optimal wing aspect ratio

Fig. 9 Pareto frontiers of expected fuel burn vs probability of satisfying requirements and the optimal wing aspect ratios along the Pareto frontiers.

aircraft is the same as that given in Eq. (2) for the D8 concept aircraft, and the numerical simulation model is also TASOPT. We again apply the multi-information source approach to generate the Pareto frontier of the expected fuel burn versus the risk of not satisfying the performance requirements for the advanced-technology 737 aircraft, and the results are shown in Fig. 9a. Like the D8 concept aircraft, the advanced-technology 737 also relatively insensitive to the uncertainties.

Similarly, we consider a hypothetical advanced-technology 777 aircraft. Like the advanced-technology 737 aircraft, it is outfitted with the same advanced technologies as the D8 concept aircraft but has a conventional fuselage and two engines under the wings. Therefore, it is also assumed to have the same uncertain model parameters as those listed in Table 2, except for the fuselage boundary-layer ingestion fraction parameter. However, the advanced-technology 777 aircraft is sized for 450 passengers and 6000 n mile range. Thus, the span length requirement in Eq. (1) is increased from 117.5 to 200 ft to reflect the larger class. The Pareto frontier for this aircraft is also shown in Fig. 9a. It can be seen that, compared to the D8 concept aircraft and the advanced-technology 737 aircraft, the advanced-technology 777 aircraft needs to trade off more expected fuel burn to satisfy performance requirements. In this study, the larger aircraft is more sensitive to the uncertainties in the technologies that underlie its performance.

V. Conclusions

This paper presented a Monte Carlo multi-information source approach for solving an aircraft conceptual design problem with uncertainties in the projections of technological improvements. Given the modeling assumptions and the assessment of the uncertainties, the expected fuel burn for a concept D8 design decreased from 2.69 to 2.43 $\mathrm{kJ}/(\mathrm{kg} \cdot \mathrm{km})$, whereas the probability of satisfying the performance requirements increased from 22 to 84% by taking into account the uncertainties in the design process. This is facilitated by our information-reuse estimator that reduces the computational cost relative to the regular Monte Carlo estimator by 90%. It makes use of the correlation between the random output of the aircraft model induced by the uncertain model parameters at different points in the design space. In other words, considering the model output as a random process indexed by the design variables, the information-reuse estimator is in effect taking advantage of the autocorrelation structure of the model in the design space and generates the desired statistics with less computational effort.

The multi-information source approach developed based on the information-reuse estimator is suitable to a broad range of other optimization under uncertainty problems because it is nonintrusive, easily parallelizable, and can handle a large number of uncertain model parameters with arbitrary probability distributions. Because it is based on Monte Carlo simulation, it is broadly applicable with few assumptions; the variance of the model output has to be finite. If the mathematical model is not smooth in the design space, the correlation between the model outputs at neighboring design points may be low. Furthermore, because the correlation between the model outputs tends to be higher when the design points are close together, an optimization routine that samples the design space widely for many optimization iterations before converging to a design point may not realize the benefit of the information-reuse estimator until the design points start to cluster. In either situation, the safeguard mechanism would fall back to regular Monte Carlo estimation so that the process would not be worse off than performing regular Monte Carlo estimation.

Finally, by carrying forward the database of past estimators and estimator variances, it was demonstrated that the multi-information source approach can be adapted to further reduce the computational cost of solving multiple optimization under uncertainty problems, enabling the trade off between risk and performance in the optimal aircraft designs.

Acknowledgments

This work was supported by the U.S. Air Force Office of Scientific Research Multidisciplinary University Research Initiative on Uncertainty Quantification, grant FA9550-09-0613, program manager F. Fahroo. The authors thank M. Drela for use of the Transport Aircraft System Optimization design tool and for advice on the aircraft design studies.

References

[1] Greitzer, E. M., Bonnefoy, P. A., de la Rosa Blanco, E., Dorbian, C. S., Drela, M., Hall, D. K., Hansman, R. J., Hileman, J. I., Liebeck, R. H., Lovegren, J., Mody, P., Pertuze, J. A., Sato, S., Spakovszky, Z. S., Tan, C. S., Hollman, J. S., Duda, J. E., Fitzgerald, N., Houghton, J., Kerrebrock, J. L., Kiwada, G. F., Kordonowy, D., Parrish, J. C., Tylko, J., Wen, E. A., and Lord, W. K., "$N + 3$ Aircraft Concept Designs and Trade Studies, Volume 1," NASA CR-2010-216794/VOL1, 2010.

[2] Drela, M., "Design Drivers of Energy-Efficient Transport Aircraft," *SAE International Journal of Aerospace*, Vol. 4, No. 2, 2011, pp. 602–618. doi:10.4271/2011-01-2495

[3] Schmit, L. A., "Structural Synthesis—Its Genesis and Development," *AIAA Journal*, Vol. 19, No. 10, 1981, pp. 1249–1263. doi:10.2514/3.7859

[4] Mavris, D. N., Bandte, O., and DeLaurentis, D. A., "Robust Design Simulation: A Probabilistic Approach to Multidisciplinary Design," *Journal of Aircraft*, Vol. 36, No. 1, 1999, pp. 298–307. doi:10.2514/2.2437

[5] Queipo, N. V., Haftka, R. T., Shyy, W., Goel, T., Vaidyanathan, R. V., and Tucker, P. K., "Surrogate-Based Analysis and Optimization," *Progress in Aerospace Sciences*, Vol. 41, No. 1, 2005, pp. 1–28. doi:10.1016/j.paerosci.2005.02.001

[6] Eldred, M. S., Giunta, A. A., Wojtkiewicz, S. F. Jr., and Trucano, T. G., "Formulations for Surrogate-Based Optimization Under Uncertainty," *9th AIAA/ISSMO Symposium on Multidisciplinary Analysis and Optimization*, AIAA Paper 2002-5585, Sept. 2002.

[7] Eldred, M. S., "Design Under Uncertainty Employing Stochastic Expansion Methods," *International Journal for Uncertainty Quantification*, Vol. 1, No. 2, 2011, pp. 119–146. doi:10.1615/IntJUncertaintyQuantification.v1.i2

[8] Ng, L. W. T., "Multifidelity Approaches for Design Under Uncertainty," Ph.D. Thesis, Massachusetts Inst. of Technology, Cambridge, MA, 2013.

[9] Ng, L. W. T., and Willcox, K. E., "Multifidelity Approaches for Optimization Under Uncertainty," *International Journal for Numerical Methods in Engineering*, Vol. 100, No. 10, 2014, pp. 746–772. doi:10.1002/nme.v100.10

[10] Hammersley, J. M., and Handscomb, D. C., *Monte Carlo Methods*, Methuen, London, 1964.

[11] Nelson, B. L., "On Control Variate Estimators," *Computers & Operations Research*, Vol. 14, No. 3, 1987, pp. 219–225. doi:10.1016/0305-0548(87)90024-4

[12] Giles, M. B., "Multilevel Monte Carlo Path Simulation," *Operations Research*, Vol. 56, No. 3, 2008, pp. 607–617. doi:10.1287/opre.1070.0496

[13] Speight, A., "A Multilevel Approach to Control Variates," *Journal of Computational Finance*, Vol. 12, No. 4, 2009, pp. 3–27.

[14] Boyaval, S., and Lelièvre, T., "A Variance Reduction Method for Parametrized Stochastic Differential Equations Using the Reduced Basis Paradigm," *Communications in Mathematical Sciences*, Vol. 8, No. 3, 2010, pp. 735–762. doi:10.4310/CMS.2010.v8.n3.a7

[15] Boyaval, S., "A Fast Monte-Carlo Method with a Reduced Basis of Control Variates Applied to Uncertainty Propagation and Bayesian Estimation," *Computer Methods in Applied Mechanics and Engineering*, Vol. 241, Oct. 2012, pp. 190–205. doi:10.1016/j.cma.2012.05.003

[16] Tracey, B., Wolpert, D., and Alonso, J. J., "Using Supervised Learning to Improve Monte Carlo Integral Estimation," *AIAA Journal*, Vol. 51, No. 8, 2013, pp. 2015–2023. doi:10.2514/1.J051655

[17] Greitzer, E. M., Bonnefoy, P. A., de la Rosa Blanco, E., Dorbian, C. S., Drela, M., Hall, D. K., Hansman, R. J., Hileman, J. I., Liebeck, R. H., Lovegren, J., Mody, P., Pertuze, J. A., Sato, S., Spakovszky, Z. S., Tan, C. S., Hollman, J. S., Duda, J. E., Fitzgerald, N., Houghton, J., Kerrebrock, J. L., Kiwada, G. F., Kordonowy, D., Parrish, J. C., Tylko, J., Wen, E. A., and Lord, W. K., "$N + 3$ Aircraft Concept Designs and Trade Studies, Volume 2, Design Methodologies for Aerodynamics,

Structures, Weight, and Thermodynamic Cycles," NASA CR-2010-216794/VOL2, 2010.

[18] "Excrescence Drag Levels on Aircraft," Engineering Sciences Data Unit (ESDU) TR-94044, 2007.

[19] Horlock, J. H., Watson, D. T., and Jones, T. V., "Limitations on Gas Turbine Performance Imposed by Large Turbine Cooling Flows," *Journal of Engineering for Gas Turbines and Power*, Vol. 123, No. 3, 2001, pp. 487–494. doi:10.1115/1.1373398

[20] Sargison, J. E., Guo, S. M., Oldfield, M. L. G., Lock, G. D., and Rawlinson, A. J., "A Converging Slot-Hole Film-Cooling Geometry—Part 2: Transonic Nozzle Guide Vane Heat Transfer and Loss," *Journal of Turbomachinery*, Vol. 124, No. 3, 2002, pp. 461–471. doi:10.1115/1.1459736

[21] Garthwaite, P. H., Kadane, J. B., and O'Hagan, A., "Statistical Methods for Eliciting Probability Distributions," *Journal of the American Statistical Association*, Vol. 100, No. 470, 2005, pp. 680–701. doi:10.1198/016214505000000105

[22] Knuth, D. E., *The Art of Computer Programming, Vol. 2: Seminumerical Algorithms*, 3rd ed., Addison–Wesley, Reading, MA, 1998.

[23] Kim, I. Y., and de Weck, O. L., "Adaptive Weighted Sum Method for Multiobjective Optimization: A New Method for Pareto Front Generation," *Structural and Multidisciplinary Optimization*, Vol. 31, No. 2, 2006, pp. 105–116. doi:10.1007/s00158-005-0557-6

[24] Das, I., and Dennis, J. E., "Normal-Boundary Intersection: A New Method for Generating the Pareto Surface in Nonlinear Multicriteria Optimization Problems," *SIAM Journal on Optimization*, Vol. 8, No. 3, 1998, pp. 631–657. doi:10.1137/S1052623496307510

[25] Powell, M. J. D., "A Direct Search Optimization Method that Models the Objective and Constraint Functions by Linear Interpolation," *Advances in Optimization and Numerical Analysis*, Vol. 275, Mathematics and Its Applications, Springer, The Netherlands, 1994, pp. 51–67. doi:10.1007/978-94-015-8330-5

[26] Conn, A. R., Scheinberg, K., and Vicente, L. N., *Introduction to Derivative-Free Optimization*, Soc. for Industrial and Applied Mathematics, Philadelphia, 2009.